

# Improving Graph Neural Network Training, Defense and Hypergraph Partitioning via Adversarial Robustness Evaluation

Yongyu Wang

**Abstract.** Graph Neural Networks (GNNs) are a highly effective neural network architecture for processing graph-structured data. Unlike traditional neural networks that rely solely on the features of the data as input, GNNs leverage both the graph structure, which represents the relationships between data points, and the feature matrix of the data to optimize their feature representation. This unique capability enables GNNs to achieve superior performance across various tasks. However, it also makes GNNs more susceptible to noise and adversarial attacks from both the graph structure and data features, which can significantly increase the training difficulty and degrade their performance. Similarly, a hypergraph is a highly complex structure, and partitioning a hypergraph is a challenging task. This paper leverages spectral adversarial robustness evaluation to effectively address key challenges in complex-graph algorithms. By using spectral adversarial robustness evaluation to distinguish robust nodes from non-robust ones and treating them differently, we propose a training-set construction strategy that improves the training quality of GNNs. In addition, we develop algorithms to enhance both the adversarial robustness of GNNs and the performance of hypergraph partitioning. Experimental results show that this series of methods is highly effective.

## 1 Introduction

The rise of Graph Neural Networks (GNNs) has brought about a transformative shift in the field of machine learning, particularly for tasks involving graph-structured data [1–4]. These networks have demonstrated success across a wide array of real-world scenarios, including recommendation systems [5], traffic forecasting [6], chip design [7], language processing [8] and social network analytics [9]. The unique advantage of GNNs lies in their ability to effectively leverage the graph that represents the relationships between data points to optimize their feature representations. This enables GNNs to fully utilize the crucial graph topology inherent in graph-structured data, unlike traditional neural networks, which optimize data representations based solely on feature vectors, thus overlooking the valuable graph structure.

However, like other neural networks, GNNs are susceptible to noise and adversarial attacks in the graph and feature space [10, 11]. Research has shown

---

Correspondence to: yongyuw@mtu.edu

that even slight modifications to the graph—such as adding, removing, or rearranging a small number of edges—can significantly impact the performance of GNNs [12, 13].

To address this issue, researchers have proposed various methods to reduce the impact of noise on the model’s performance. These approaches can be divided into two categories: reactive and proactive defenses. Reactive defenses focus on identifying adversarial examples within the model’s inputs, as explored in previous studies [14–16]. On the other hand, proactive defenses aim to strengthen the model’s robustness, making it less susceptible to adversarial attacks, as demonstrated by methods proposed in works such as [17, 18].

However, due to the diversity of noise types and model structures, developing effective methods to defend against noise across various scenarios remains a significant challenge. Unlike existing approaches that focus on mitigating the effects of noise, we argue that, given the inevitability of noise, the focus should shift toward how to better leverage it. From this new perspective, this paper proposes a framework that first identifies the most noise-sensitive training samples and then uses these samples to construct a smaller but more effective training set for training the GNN model. This approach enhances the model’s ability to correctly process noisy data.

In this work, we also propose a new approach to improve the defense ability of GNNs. Specifically, we apply spectral adversarial robustness evaluation to partition nodes in the graph into two groups: robust nodes that are relatively insensitive to noise and perturbations, and non-robust nodes that are more easily affected. We then treat these two groups differently. For robust nodes, we induce a subgraph containing only them from the original graph, and use a GNN to predict their class labels. For non-robust nodes, we leverage the topology of the original graph to propagate class information from robust nodes to obtain their labels.

We also provide an efficient high performance hypergraph partitioning method based on spectral adversarial robustness evaluation and demonstrate its effectiveness on benchmark VLSI data sets.

## 2 Preliminaries

### 2.1 The Vulnerability of GNNs to noise and adversarial attacks

The vulnerability of Graph Neural Networks (GNNs) to noise and adversarial attacks refers to the difficulty GNNs face in maintaining consistent outputs when exposed to perturbations in the graph structure, such as the presence of incorrect or redundant edges in the input graph, or errors in the feature representations within the input feature matrix. [19] investigated the task- and model-agnostic vulnerabilities of GNNs, showing that these networks are very vulnerable to adversarial perturbations, regardless of the downstream task.

## 2.2 Spectral Graph Theory

Spectral Graph Theory is a mathematical method that uses the eigenvalues and eigenvectors of the Laplacian matrix of a graph to study its properties. Given a graph  $G = (V, E, w)$ , where  $V$  represents the set of vertices,  $E$  is the set of edges, and  $w$  is a function assigning positive weights to each edge. The Laplacian matrix of graph  $G$ , which is a symmetric diagonally dominant (SDD) matrix, is defined as follows:

$$L(p, q) = \begin{cases} -w(p, q) & \text{if } (p, q) \in E, \\ \sum_{(p, t) \in E} w(p, t) & \text{if } p = q, \\ 0 & \text{otherwise.} \end{cases} \quad (1)$$

For better numerical stability and to make the Laplacian matrix scale-invariant, the normalized Laplacian matrix  $L_{\text{norm}}$  can be computed as:

$$L_{\text{norm}} = D^{-1/2} L D^{-1/2}$$

According to spectral graph theory, analyzing a graph often requires only one or a few specific eigenvalues and their corresponding eigenvectors [20]. For example, when analyzing the clustering structure of a graph using spectral graph theory, only the smallest eigenvalues and their corresponding eigenvectors are useful [21]. Therefore, for a Laplacian matrix, it is unnecessary to compute all the eigenpairs through direct eigen decomposition, and for a large-scale graph, the computational cost would be too high. The Courant-Fischer Minimax Theorem [22] allows the eigenvalues to be computed iteratively without explicitly calculating all the eigenvalues. Specifically:

The  $k$ -th largest eigenvalue of the Laplacian matrix  $L \in \mathbb{R}^{|V| \times |V|}$  can be computed as follows:

$$\lambda_k(L) = \min_{\dim(U)=k} \max_{x \in U, x \neq 0} \frac{x^T L x}{x^T x}$$

In many practical applications, the problem-solving process involves not just a single matrix, but rather the relationship between two matrices. Therefore, the Courant-Fischer Minimax Theorem is extended to the generalized case, resulting in the following Generalized Courant-Fischer Minimax Theorem:

Consider two Laplacian matrices  $L_X \in \mathbb{R}^{|V| \times |V|}$  and  $L_Y \in \mathbb{R}^{|V| \times |V|}$ , where it holds that  $\text{null}(L_Y) \subseteq \text{null}(L_X)$ . Under the condition  $1 \leq k \leq \text{rank}(L_Y)$ , the  $k$ -th largest eigenvalue of the matrix  $L_Y^+ L_X$  can be computed as follows:

$$\lambda_k(L_Y^+ L_X) = \min_{\dim(U)=k, U \perp \text{null}(L_Y)} \max_{x \in U} \frac{x^T L_X x}{x^T L_Y x}$$

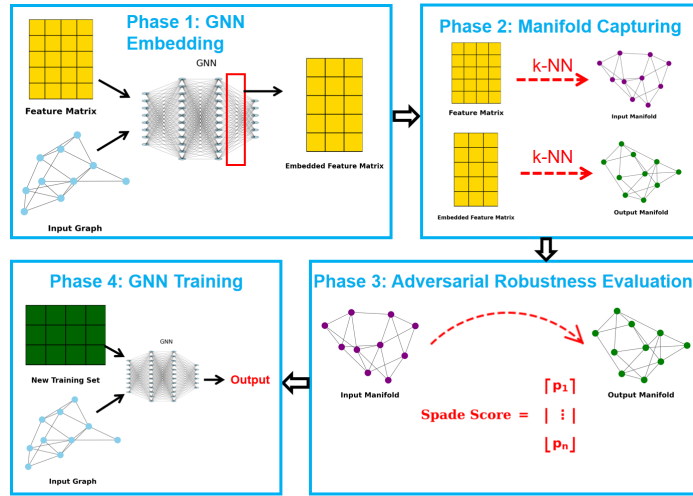


Fig. 1: Overview of the proposed method.

### 3 Improving Graph Neural Network Training

#### 3.1 Method

Figure 1 shows the proposed method for training GNNs using top non-robust training samples in the training set, which consists of four key phases: Phase (1) is GNN embedding, which uses the original input to train a GNN and takes the output of the hidden layer as the embedding result of the data’s feature matrix; In Phase (2), we use k-NN graphs to capture the underlying manifolds of the input feature matrix and the embedded feature matrix; In Phase (3), we calculate each node’s level of non-robustness using the input manifold and the output manifold; In Phase (4), we use the top non-robust samples selected from the training set to train the GNN. In the rest of this section, we provide a detailed description of these four phases.

**Phase 1: GNN Embedding** [23] proposed leveraging a bijective distance mapping between the manifolds of a model’s input and output data to analyze the adversarial robustness of each data point for a given model.

To obtain the output data of the GNN model, we first train the GNN using the original feature matrix and input graph. Once trained, the GNN is then used to transform the input feature matrix. Since the final layer of a GNN is typically task-specific—such as a softmax layer for multi-class classification tasks—we take the output of the hidden layer before the final output layer as the embedding result.

**Phase 2: Manifold Capturing** The manifold of the data is typically captured using graphs, and k-nearest neighbor graphs are the most widely used for

this purpose. In this phase, we use k-nearest neighbor (k-NN) graphs to capture the underlying manifolds of the input feature matrix and the embedded feature matrix. The conventional k-NN graph construction algorithm exhibits a time complexity of  $O(|N|^2)$ , where  $|N|$  is the total number of nodes in the graph. Such quadratic complexity makes it impractical for large-scale datasets. To overcome this limitation, an approximate kNN graph construction algorithm can be employed [24]. This approach leverages an extension of the probabilistic skip list structure to achieve a reduced time complexity of  $O(|N| \log |N|)$ , which is more suitable for large-scale data processing.

**Phase 3: Adversarial Robustness Evaluation** Let  $L_X$  and  $L_Y$  denote the Laplacian matrices corresponding to the k-NN graphs of the input feature matrix and the embedded feature matrix constructed in phase 2, respectively. Building on the theoretical framework introduced in [23], we leverage the largest generalized eigenvalues and their associated eigenvectors of  $L_Y^+ L_X$  to assess the robustness of each individual sample to noise during the processing by a given model. Specifically, we calculate the weighted eigensubspace matrix  $V_s \in \mathbb{R}^{|V| \times s}$  to perform spectral embedding of the input manifold  $G_X = (V, E_X)$ , where  $|V|$  represents the total number of nodes. The matrix  $V_s$  is expressed as:

$$V_s = [v_1 \sqrt{\zeta_1}, v_2 \sqrt{\zeta_2}, \dots, v_s \sqrt{\zeta_s}],$$

where  $\zeta_1 \geq \zeta_2 \geq \dots \geq \zeta_s$  are the top  $s$  eigenvalues of  $L_Y^+ L_X$ , and  $v_1, v_2, \dots, v_s$  are the corresponding eigenvectors.

Using  $V_s$ , we project the nodes of  $G_X$  into an  $s$ -dimensional space, representing each node  $p$  as the  $p$ -th row of  $V_s$ . According to [23], the stability of an edge  $(p, q) \in E_X$  is quantified by computing the spectral embedding distance between nodes  $p$  and  $q$ :

$$\|V_s^\top e_{p,q}\|_2^2.$$

To assess the robustness of a node  $p$ , a metric referred to as the *Spade score* is defined as the average embedding distance to the neighbors within the input manifold:

$$\text{Spade}(p) = \frac{1}{|N_X(p)|} \sum_{q \in N_X(p)} \|V_s^\top e_{p,q}\|_2^2,$$

where  $N_X(p)$  represents the set of neighbors of node  $p$  in  $G_X$ . A higher  $\text{Spade}(p)$  value suggests that node  $p$  is more prone to adversarial attacks.

**Phase 4: GNN Training** For the samples in the training set, we rank them in descending order based on their Spade scores and select the top portion to form a new, smaller training set. The points in this new training set are those that are highly susceptible to noise and likely to mislead the GNN. By training the GNN using only these noise-sensitive samples, we are effectively enhancing the GNN’s ability to resist being misled by such samples.

### 3.2 Experiments

We have evaluated our framework on three of the most popular GNN models and three classic benchmark datasets.

**Data Sets** We evaluate the proposed method on three standard citation network benchmarks, where nodes represent documents, edges correspond to citations, and each node is associated with a sparse bag-of-words feature vector and a class label. The key statistics of these datasets are summarized in Table 1.

- **Cora**: A dataset of scientific publications categorized into seven classes.
- **Citeseer**: A dataset of scientific publications that is sparser than Cora and exhibits a more uneven class distribution, making it more challenging for graph-based classification methods.
- **PubMed**: A large biomedical dataset where nodes are represented by TF-IDF word vectors from a 500-word vocabulary.

Table 1: Statistics of datasets used in our experiments.

Dataset	Nodes	Edges	Classes	Features
Cora	2,708	5,429	7	1,433
Citeseer	3,327	4,732	6	3,703
PubMed	19,717	44,338	3	500

**GNN Models** We use the following three commonly used GNN models for our experiments:

- **Graph Convolutional Network (GCN)**: A widely used model that applies convolution-like operations to graph-structured data by aggregating information from neighboring nodes using a layer-wise propagation rule.
- **Graph Attention Network (GAT)**: Introduces an attention mechanism to assign different importance weights to neighboring nodes during the message-passing process.
- **GraphSAGE**: An inductive model that learns aggregation functions to generate node embeddings by sampling and aggregating features from a fixed number of neighboring nodes.

### Detailed Model Implementation and Parameter Settings

- **GCN:** We use the same GCN architecture and parameter settings for all three datasets. The model consists of two graph convolutional layers: the first layer transforms node features to a 64-dimensional space, and the second layer maps them to the number of output classes, with ReLU activation applied after the first convolution. For the Cora dataset, the learning rate is set to 0.01. For the Citeseer and PubMed datasets, it is set to 0.1.
- **GAT:** For the Cora dataset, the GAT model consists of two layers: the first layer has 4 attention heads with 8 hidden units each, followed by an ELU activation, and the second layer has 1 attention head that outputs the number of class logits. For the Citeseer dataset, the GAT model also has two layers: the first layer uses 8 attention heads with 8 hidden units each, followed by an ELU activation, and the second layer has 1 attention head that outputs the class logits. For the PubMed dataset, the GAT model has the same structure as the Citeseer model but includes layer normalization after each layer and uses a Leaky ReLU activation after the first layer. For the Cora dataset, the learning rate is set to 0.01. For the Citeseer dataset, it is set to 0.1, and for the PubMed dataset, it is set to 0.05.
- **GraphSAGE:** The GraphSAGE architecture for the Cora and Citeseer datasets consists of two layers: the first layer uses **SAGEConv** with 64 hidden units, followed by batch normalization, ReLU activation, and a dropout layer with a probability of 0.5. The second layer uses **SAGEConv** with 64 input features and outputs the class labels. The architecture for the PubMed dataset also consists of two layers, but the first layer uses **SAGEConv** with 32 hidden units, followed by batch normalization, ReLU activation, and a dropout layer. The second layer uses **SAGEConv** with 32 input features and outputs the class labels. For all three datasets, the learning rate is set to 0.05.

For all the experiments, the Adam optimizer is used with a weight decay of  $5 \times 10^{-4}$ , and the loss function for multi-class classification is CrossEntropyLoss. The number of eigenvectors is set to 10, and the value of  $k$  in k-NN is set to 20.

**Results** We first perform an 80-20 split of the entire dataset by randomly sampling 80% of the samples to form the original full training set and using the remaining 20% as the test set. Then, we construct two different types of training sets: (1) forming the training set by selecting the top 80% of non-robust samples from the original full training set using our method; (2) forming the training set by randomly sampling 80% of the original full training set.

We train the GNN models using the original full training set and the two smaller training sets mentioned above, and the classification accuracy across different epochs is shown in Table 2. In these charts, **Random** represents the training set constructed by randomly sampling 80% of the original full training set, **Ours** represents the training set constructed using our method, and **Full** represents the original full training set.

From the experimental results, it can be observed that in all 9 combinations of the three GNN models and the three datasets, the training set constructed

using our method achieved the highest classification accuracy after 5 epochs of training. Moreover, the advantage of our method is particularly evident on the largest dataset, PubMed. On PubMed, our method outperforms the second-best method by **14.1%**, **7.4%**, and **3.4%** in accuracy for the GCN, GAT, and GraphSAGE models, respectively.

Our method not only significantly outperforms the randomly sampled training sets of the same size but also demonstrates substantial advantages compared to the full training sets, which are 20% larger, highlighting the effectiveness of our approach. The experimental results further show that randomly selecting 80% of the training samples from the full training set yields almost no difference in performance compared to using the full set. However, when 80% of the samples are selected using our method, which prioritizes the most non-robust nodes, the training performance is significantly improved. This demonstrates that focusing on non-robust samples during training, rather than uniformly sampling all nodes, enables the model to better adapt to unavoidable noise, resulting in superior performance on the test set.

## 4 Improving Hypergraph partitioning

In this section, we propose a robustness-aware hypergraph partitioning framework. We first identify and extract a robust sub-hypergraph consisting of vertices that are empirically less sensitive to perturbations, and perform the partitioning algorithm only on this reduced structure. The resulting partition labels are then propagated to the remaining non-robust vertices by exploiting the underlying graph topology. In this way, our method reduces the effective size of the hypergraph (in terms of the number of vertices) while largely avoiding the degradation in solution quality that typically arises from changes to the hypergraph topology. The main contributions of this paper are summarized as follows:

- We propose a novel robustness-aware hypergraph partitioning method that leverages adversarial robustness evaluation to distinguish robust nodes from non-robust nodes and treats them differently during the partitioning process.
- We propose a highly novel label propagation scheme for propagating partition labels within hypergraphs.
- We conduct extensive experiments on diverse hypergraph instances extracted from realistic VLSI design problems and demonstrate that our approach achieves clearly improved performance over existing hypergraph coarsening methods.

### 4.1 Method

Our method is built on the key idea of treating nodes that are robust to perturbations separately from those that are vulnerable. For nodes that are less susceptible to perturbations, we directly apply a hypergraph partitioning algorithm to obtain their partitions. In contrast, for nodes that are more easily

Table 2: Classification Accuracy Across Epochs for GCN, GAT, and GraphSAGE on Cora, Citeseer, and PubMed

Model	Dataset	Training Set	Epoch 1	Epoch 2	Epoch 3	Epoch 4	Epoch 5
GCN	Cora	Random	0.2939	0.3290	0.5360	0.7209	0.7671
		Ours	0.5416	0.6580	0.6525	0.7375	<b><u>0.8041</u></b>
		Full	0.2939	0.3290	0.5527	0.7227	<b><u>0.8041</u></b>
	Citeseer	Random	0.2331	0.6030	0.6030	0.6256	0.6256
		Ours	0.4797	0.5278	0.5609	0.6316	<b><u>0.6947</u></b>
		Full	0.2406	0.5925	0.5925	0.6541	0.6541
	PubMed	Random	0.3918	0.4420	0.5836	0.6191	0.6191
		Ours	0.3974	0.5181	0.7515	0.8052	<b><u>0.8080</u></b>
		Full	0.3921	0.4484	0.6082	0.6082	0.6670
GAT	Cora	Random	0.3124	0.3623	0.4603	0.6488	0.7634
		Ours	0.4954	0.6007	0.6506	0.7726	<b><u>0.8299</u></b>
		Full	0.3216	0.3604	0.4713	0.6654	0.7782
	Citeseer	Random	0.6451	0.6451	0.6451	0.6917	0.6917
		Ours	0.5594	0.5504	0.6105	0.7053	<b><u>0.7504</u></b>
		Full	0.6331	0.6331	0.6617	0.7158	0.7158
	PubMed	Random	0.4027	0.4603	0.5787	0.5787	0.5787
		Ours	0.4174	0.3977	0.4154	0.5580	<b><u>0.6528</u></b>
		Full	0.3987	0.4415	0.5455	0.5455	0.5455
GraphSAGE	Cora	Random	0.4824	0.7689	0.7745	0.7893	0.8041
		Ours	0.4991	0.7006	0.7486	0.8115	<b><u>0.8244</u></b>
		Full	0.4880	0.7745	0.7837	0.8059	<b><u>0.8244</u></b>
	Citeseer	Random	0.4797	0.6737	0.6902	0.7038	0.7113
		Ours	0.4857	0.6451	0.6692	0.7188	<b><u>0.7624</u></b>
		Full	0.4812	0.6872	0.6872	0.6992	0.7218
	PubMed	Random	0.3974	0.6429	0.7406	0.7697	0.7735
		Ours	0.3977	0.5945	0.6523	0.7210	<b><u>0.8078</u></b>
		Full	0.3974	0.6378	0.7484	0.7652	0.7662

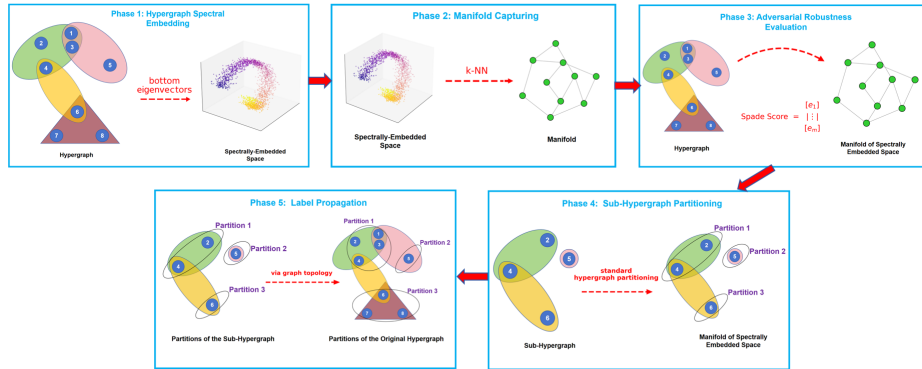


Fig. 2: Overview of the proposed method.

affected by such perturbations, we do not rely on hypergraph spectral partitioning; instead, we infer their partition membership based on their relationships with the robust nodes and propagate the partitioning results from the robust subset to these vulnerable nodes. Specifically, as shown in Figure 2, our method consists of the following five phases.

**Phase 1: Hypergraph Spectral Embedding** We first perform a spectral embedding of the hypergraph by mapping it into the feature space spanned by the  $K$  eigenvectors of its Laplacian matrix corresponding to the smallest eigenvalue magnitudes.

**Phase 2: Manifold Capturing** Data manifolds are commonly modeled using graphs, with  $k$ -nearest neighbor ( $k$ -NN) graphs being one of the most prevalent choices. In this stage, we construct a  $k$ -NN graph to capture the underlying manifold structure of the spectrally embedded hypergraph. A standard  $k$ -NN construction procedure has a time complexity of  $O(|N|^2)$ , where  $|N|$  denotes the number of nodes, which becomes prohibitive for large-scale datasets. To address this issue, we adopt an approximate  $k$ -NN graph construction algorithm [24], which extends a probabilistic skip-list-like structure and reduces the complexity to  $O(|N| \log |N|)$ , making it far more suitable for large-scale data processing.

**Phase 3: Adversarial Robustness Evaluation** Let  $L_X$  and  $L_Y$  denote the Laplacian matrices associated with the hypergraph  $H$  and the  $k$ -NN graph constructed from the spectrally embedded hypergraph in phase 2, respectively. Following the theoretical framework in [23], we exploit the dominant generalized eigenvalues of  $L_Y^+ L_X$  and their corresponding eigenvectors to characterize the sensitivity of each sample to noise under a given model. In particular, we compute a weighted eigensubspace matrix  $V_s \in \mathbb{R}^{|V| \times s}$  to obtain a spectral embedding of the input manifold  $G_X = (V, E_X)$ , where  $|V|$  is the number of nodes.

The matrix  $V_s$  is defined as

$$V_s = [v_1\sqrt{\zeta_1}, v_2\sqrt{\zeta_2}, \dots, v_s\sqrt{\zeta_s}],$$

where  $\zeta_1 \geq \zeta_2 \geq \dots \geq \zeta_s$  are the largest  $s$  eigenvalues of  $L_Y^\dagger L_X$ , and  $v_1, v_2, \dots, v_s$  are the associated eigenvectors.

Using  $V_s$ , each node  $p$  in  $G_X$  is mapped to an  $s$ -dimensional representation given by the  $p$ -th row of  $V_s$ . As described in [23], the stability of an edge  $(p, q) \in E_X$  can then be measured by the spectral embedding distance between nodes  $p$  and  $q$ :

$$\|V_s^\top e_{p,q}\|_2^2.$$

To quantify the robustness of a node  $p$ , a score termed the *Spade score* is introduced as the average embedding distance to its neighbors on the input manifold:

$$\text{Spade}(p) = \frac{1}{|N_X(p)|} \sum_{q \in N_X(p)} \|V_s^\top e_{p,q}\|_2^2,$$

where  $N_X(p)$  denotes the neighbor set of node  $p$  in  $G_X$ . A larger value of  $\text{Spade}(p)$  indicates that node  $p$  is more vulnerable to adversarial perturbations.

## 4.2 Phase 4: Sub-Hypergraph Partitioning

For the nodes in the hypergraph  $H$  we first sort them in descending order according to their Spade scores and select the bottom portion to form the robust node set. Using these robust nodes together with the hyperedges that connect them in the original hypergraph, we construct a robust sub-hypergraph. We then apply a standard hypergraph partitioning algorithm to this sub-hypergraph to obtain a partition of the robust nodes.

## 4.3 Label Propagation from Robust to Non-Robust Nodes

The nodes that are not included in the robust node set are referred to as non-robust nodes. Since these nodes are vulnerable to adversarial perturbations and attacks that affect hypergraph spectral partitioning, we do not directly apply the hypergraph spectral partitioning algorithm to determine their partitions. Instead, we infer their partition membership based on their relationships with the robust nodes, effectively propagating the partitioning result from the robust subset to the non-robust nodes. Specifically, for each non-robust node, we identify the robust node with which it co-occurs in hyperedges in  $H$  most frequently, and assign the non-robust node to the same partition as that robust node.

The complete algorithm of the proposed method has been shown in Algorithm 1.

**Algorithm 1** Robust Hypergraph Partitioning**Input:** A hypergraph  $H = (V, E)$ **Output:** Partitioned hypergraph.

- 1: Extract the adjacency matrix  $A$  from the input hypergraph  $H$ .
- 2: Compute the Laplacian matrix  $\mathbf{L}_H$  for the graph  $H$ .
- 3: Compute the eigenvectors  $u_1, \dots, u_k$  that correspond to the bottom  $k$  nonzero eigenvalues of  $A$ ;
- 4: Construct  $U \in \mathbb{R}^{n \times k}$ , with  $k$  eigenvectors of  $A$  stored as columns;
- 5: Construct a  $k$ -nearest neighbor graph  $G = (V, E)$  from  $U$ .
- 6: Compute the Laplacian matrix  $\mathbf{L}_U$  for the graph  $U$ .
- 7: Compute the SPADE score of each node.
- 8: Form a robust node set from nodes with small SPADE scores, while constructing a non-robust node set from nodes with large SPADE scores.
- 9: Construct a sub-hypergraph  $S$  consisting of the robust node set and all hyperedges in  $H$  that connect only these robust nodes.
- 10: For each non-robust node, count the number of hyperedges in  $H$  where it appears together with each robust node.
- 11: Apply standard hypergraph spectral partitioning on  $S$ .
- 12: For each non-robust node, identify the robust node with which it co-occurs in hyperedges in  $H$  most frequently, and assign the non-robust node to the partition containing that robust node.
- 13: Return the partitioned hypergraph.

Table 3: The average local conductance ( $\Phi$ ) comparison between our methods and other methods

Hypergraph	V	E	Spectral S	Spectral C	Metis S	Metis C	hMETIS	HyperSF	Ours
ibm01	12752	14111	0.94	0.81	0.84	0.78	0.65	0.44	0.28
ibm02	19601	19584	0.94	0.84	0.83	0.79	0.69	0.52	0.43
ibm03	23136	27401	0.95	0.86	0.85	0.79	0.67	0.48	0.41
ibm04	27507	31970	0.95	0.84	0.84	0.78	0.68	0.47	0.40

**4.4 Experiments**

We perform extensive experiments to evaluate the performance of the proposed spectral hypergraph coarsening method on a suite of VLSI-related benchmark datasets, from “ibm01” to “ibm04”. To ensure a fair comparison, we also apply several existing hypergraph coarsening techniques to the same set of benchmarks and compare their results against ours. For brevity, we refer to the star and clique models as S and C, respectively. The experimental results are shown in Table 3. It can be seen that our method consistently outperforms all competing methods across all four datasets.

---

Datasets are available at: <https://vlscad.ucsd.edu/UCLAWeb/cheese/ispd98.html>.

## 5 Strengthen GNN Defenses via Adversarial Robustness Evaluation

In this section, we propose a method to defend GNNs using adversarially robust nodes. Specifically, we first conduct a spectral adversarial robustness evaluation and partition the nodes in the graph into two groups: adversarially robust nodes and adversarially non-robust nodes. We then extract a subgraph consisting of the adversarially robust nodes from the original graph and apply a GNN to classify these nodes. Finally, we propagate the labels from robust nodes to non-robust nodes based on the graph topology. Experiments on benchmark datasets with popular GNN architectures, evaluated under both Metattack and Nettack attacks, demonstrate that the proposed method yields highly effective defense against adversarial attacks.

### 5.1 Method

As shown in Figure 3, our method consists of six steps, which are detailed in the rest of this section.

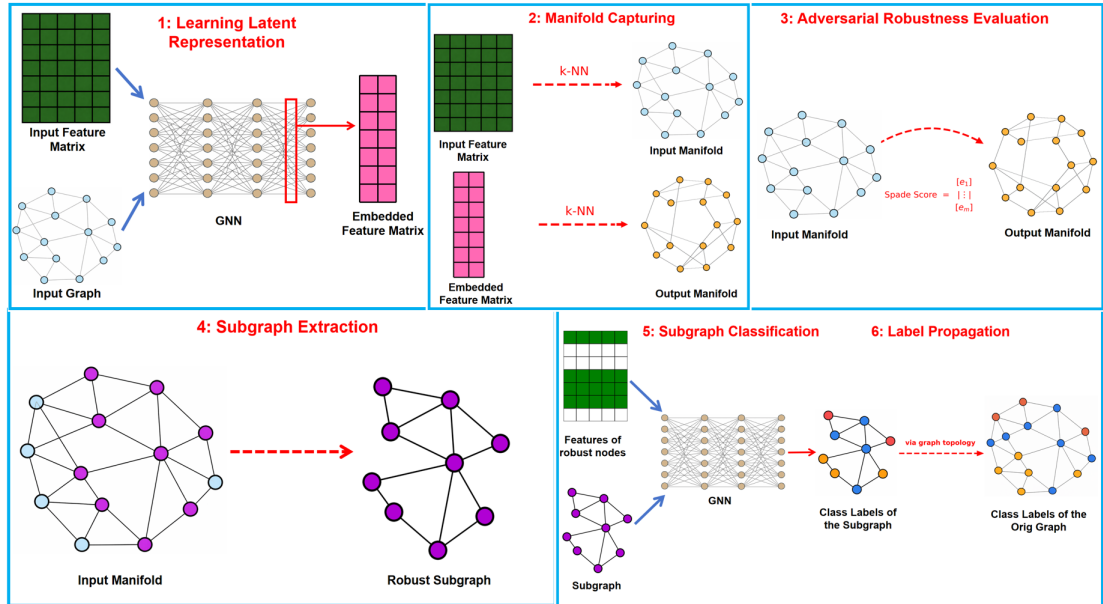


Fig. 3: Overview of the proposed method.

**Step 1: Learning Latent Representations** Machine learning models can be viewed as transformation engines that convert inputs into outputs by successively

reshaping representations. For example, deep neural networks compress and refine raw feature vectors through multiple nonlinear layers. Likewise, methods such as Support Vector Machines (SVM) and Support Vector Clustering (SVC) employ kernel functions to implicitly lift data from the original feature space into a higher-dimensional one [25]. Adversarial attacks seek to exploit this mechanism by inducing failures in the input-output transformation, causing the model to produce incorrect predictions. Therefore, we first run the model in its standard (benign) setting to obtain the model-induced transformation of the input feature space, i.e., the resulting latent representations.

**Step 2: Capturing Manifolds** The data manifold is commonly modeled using graphs. Among the many graph construction strategies, the  $k$ -nearest neighbor ( $k$ -NN) graph is one of the most widely used and is well suited for manifold approximation. Accordingly, in this phase we construct  $k$ -NN graphs to represent the manifolds of both the original input feature matrix and the embedded feature matrix obtained in Phase 1.

**Step 3: Spectral Adversarial Robustness Evaluation** Let  $L_X$  and  $L_Y$  denote the Laplacian matrices associated with the  $k$ -NN graphs built in Phase 2 from the input feature matrix and the embedded feature matrix, respectively. Following the theoretical framework in [23], we leverage the leading generalized eigenvalues of  $L_Y^+ L_X$  together with their associated eigenvectors to estimate how sensitive each sample is to noise under a specified model. Specifically, we form a weighted eigensubspace matrix  $V_s \in \mathbb{R}^{|V| \times s}$ , which serves as a spectral embedding of the input manifold  $G_X = (V, E_X)$ , where  $|V|$  denotes the number of nodes. The matrix  $V_s$  is defined as

$$V_s = [v_1 \sqrt{\zeta_1}, v_2 \sqrt{\zeta_2}, \dots, v_s \sqrt{\zeta_s}],$$

with  $\zeta_1 \geq \zeta_2 \geq \dots \geq \zeta_s$  being the top  $s$  eigenvalues of  $L_Y^+ L_X$ , and  $v_1, v_2, \dots, v_s$  the corresponding eigenvectors.

Under this construction, each node  $p$  in  $G_X$  is represented in  $\mathbb{R}^s$  by the  $p$ -th row of  $V_s$ . As stated in [23], the stability of an edge  $(p, q) \in E_X$  can be assessed via the distance between nodes  $p$  and  $q$  in the spectral embedding:

$$\|V_s^\top e_{p,q}\|_2^2.$$

To summarize node-level robustness, we adopt the Spade score, defined as the mean embedding distance from node  $p$  to its neighbors on the input manifold:

$$\text{Spade}(p) = \frac{1}{|N_X(p)|} \sum_{q \in N_X(p)} \|V_s^\top e_{p,q}\|_2^2,$$

where  $N_X(p)$  is the neighbor set of node  $p$  in  $G_X$ . A higher  $\text{Spade}(p)$  suggests that node  $p$  is more susceptible to adversarial perturbations.

**Step 4: Subgraph Extraction** For the nodes in the original graph, we first rank them in descending order by their Spade scores and then take the lowest-scoring fraction to define a robust node set. Using these robust nodes and the edges among them inherited from the original graph, we build a robust subgraph.

**Step 5: Subgraph Classification** Subsequently, we train a GNN on this robust subgraph to perform node classification for the robust nodes.

**Step 6: Label Propagation from Robust to Non-Robust Nodes** The nodes that are not included in the robust node set are referred to as non-robust nodes. Because these nodes are more susceptible to adversarial perturbations and attacks that can compromise GNN predictions, we do not apply the GNN to classify them directly. Instead, we infer their class labels from their associations with the robust nodes, i.e., we propagate the predictions obtained on the robust subset to the non-robust nodes. Concretely, for each non-robust node, we find the robust node with which it shares the largest number of connections, and assign the non-robust node to the same class as that robust node.

## 5.2 Experiments

We have evaluated our framework on three of the most popular GNN models and three classic benchmark datasets.

**Data Sets** We evaluate the proposed method on two standard citation network benchmarks, where nodes represent documents, edges encode citation links, and each node is associated with a sparse bag-of-words feature vector and a class label. A brief summary of the dataset characteristics is provided below.

- **Cora:** A citation network of 2,708 nodes and 5,429 edges, where each node is represented by a 1,433-dimensional bag-of-words feature vector and assigned to one of 7 research categories.
- **Citeseer:** A citation network of 3,327 nodes and 4,732 edges with 3,703-dimensional bag-of-words features. Compared to Cora, Citeseer is sparser and has a more imbalanced label distribution over its 6 classes, thereby posing a greater challenge for graph-based classification models.

Following ProGNN [26] and the implementation in the DeepRobust library [27], we adopt the predefined splits provided by `Dataset(..., setting="prognn")`. For each dataset, we operate on the largest connected component of the citation graph and use 10% of the nodes as labeled training data, 10% as validation data, and the remaining 80% as test data. This setting corresponds to a semi-supervised scenario with scarce labels and a relatively large test set, and is widely used in prior work on adversarial attacks and defenses on graphs [26, 27].

**GNN Models** We use the following three popular GNN models for our experiments:

- **Graph Convolutional Network (GCN):** A widely used model that applies convolution-like operations to graph-structured data by aggregating information from neighboring nodes using a layer-wise propagation rule.
- **Graph Attention Network (GAT):** Introduces an attention mechanism to assign different importance weights to neighboring nodes during the message-passing process.
- **Generalized PageRank GNN (GPR-GNN):** An architecture that combines adaptive generalized PageRank (GPR) scheme with GNNs, effectively mitigating feature over-smoothing [28].

### 5.3 Detailed Model Implementation and Parameter Settings

- **GCN:** We adopt a two-layer GCN model, where the first GCN layer maps the input node features to an 8-dimensional hidden representation, followed by a ReLU activation, and the second GCN layer projects the hidden representations to the output class space.
- **GAT:** We employ a two-layer GAT model. The first graph attention layer applies multi-head attention (with 4 heads in our experiments) to transform the input node features into an 8-dimensional hidden representation per head, whose outputs are concatenated, passed through an ELU activation. The second attention layer uses a single head without concatenation to map the hidden representations to the output class space.
- **GPR-GNN:** We adopt a GPR-GNN architecture that consists of a two-layer MLP followed by a generalized PageRank (GPR) propagation module. The MLP first maps the input node features to a 16-dimensional hidden representation using a linear layer with ReLU activation, and then uses a second linear layer to project the hidden representation to the output class logits. On top of these logits, we apply a GPR-based propagation module with  $K = 10$  propagation steps over the GCN-normalized adjacency matrix with self-loops. This module aggregates information from multiple hop distances using a set of learnable propagation coefficients, which are initialized according to a Personalized PageRank scheme with the restart probability set to 0.1.

For all experiments, we select 5% of the nodes as non-robust nodes. The number of neighbors in the  $k$ -NN graph is set to  $k = 10$ , and we use 10 eigenvectors for the spectral embedding in the adversarial robustness evaluation.

**Experimental Results** The experimental results of Metattack and Nettek are shown in Table 4 and Table 5, respectively.

Table 4: Classification accuracy (%) of three GNN models on two datasets, with and without our defense, under clean graph and Metattack. The last column reports the defense gain on attacked graphs.

Model	Dataset	Clean (Orig)	Metattack (Orig)	Clean (Ours)	Metattack (Ours)	Defense Gain
GCN	Cora	82.49	56.34	77.11	66.45	<b>10.11</b>
GCN	Citeseer	70.79	61.02	70.62	66.17	<b>5.15</b>
GAT	Cora	82.29	42.25	79.33	66.50	<b>24.25</b>
GAT	Citeseer	62.09	49.59	60.96	57.35	<b>7.76</b>
GPR-GNN	Cora	80.03	69.37	81.79	76.61	<b>7.24</b>
GPR-GNN	Citeseer	71.03	56.93	69.31	69.02	<b>12.09</b>

Table 5: Classification accuracy (%) of three GNN models on two datasets, with and without our defense, under clean graph and Nettack. The last column reports the defense gain on attacked graphs.

Model	Dataset	Clean (Orig)	Nettack (Orig)	Clean (Ours)	Nettack (Ours)	Defense Gain
GCN	Cora	82.49	62.42	77.11	74.75	<b>12.33</b>
GCN	Citeseer	64.04	53.61	65.17	63.57	<b>9.96</b>
GAT	Cora	82.49	69.97	82.04	81.89	<b>11.92</b>
GAT	Citeseer	56.64	41.59	57.41	52.13	<b>10.54</b>
GPR-GNN	Cora	74.65	60.31	68.56	67.81	<b>7.50</b>
GPR-GNN	Citeseer	67.95	58.53	68.36	66.94	<b>8.41</b>

## 6 Conclusion

This paper adopts spectral adversarial robustness evaluation to identify and select the most robust nodes from a given graph. Building on this selection, we propose three algorithms that respectively improve the training quality of GNNs, enhance the performance of hypergraph partitioning, and strengthen the adversarial robustness of GNNs against attacks. Extensive experiments demonstrate the effectiveness of all three algorithms.

## References

1. T. N. Kipf and M. Welling, “Semi-supervised classification with graph convolutional networks,” *arXiv preprint arXiv:1609.02907*, 2016.
2. P. Veličković, G. Cucurull, A. Casanova, A. Romero, P. Liò, and Y. Bengio, “Graph attention networks,” *arXiv preprint arXiv:1710.10903*, 2017.
3. Z. Hu, Y. Dong, K. Wang, K.-W. Chang, and Y. Sun, “GPT-GNN: Generative pre-training of graph neural networks,” in *Proceedings of the 26th ACM SIGKDD International Conference on Knowledge Discovery & Data Mining*, 2020, pp. 1857–1867.
4. J. Zhou, G. Cui, S. Hu, Z. Zhang, C. Yang, Z. Liu, L. Wang, C. Li, and M. Sun, “Graph neural networks: A review of methods and applications,” *AI Open*, vol. 1, pp. 57–81, 2020.

5. W. Fan, Y. Ma, Q. Li, Y. He, E. Zhao, J. Tang, and D. Yin, "Graph neural networks for social recommendation," in *Proceedings of the World Wide Web Conference*, 2019, pp. 417–426.
6. B. Yu, H. Yin, and Z. Zhu, "Spatio-temporal graph convolutional networks: A deep learning framework for traffic forecasting," *arXiv preprint arXiv:1709.04875*, 2017.
7. A. Mirhoseini *et al.*, "A graph placement methodology for fast chip design," *Nature*, vol. 594, no. 7862, pp. 207–212, 2021.
8. M. Song, Z. Zhan, and H. E., "Hierarchical schema representation for text-to-SQL parsing with decomposing decoding," *IEEE Access*, vol. 7, pp. 103706–103715, 2019.
9. R. Ying, R. He, K. Chen, P. Eksombatchai, W. L. Hamilton, and J. Leskovec, "Graph convolutional neural networks for web-scale recommender systems," in *Proceedings of the 24th ACM SIGKDD International Conference on Knowledge Discovery & Data Mining*, 2018, pp. 974–983.
10. I. Goodfellow, P. McDaniel, and N. Papernot, "Making machine learning robust against adversarial inputs," *Communications of the ACM*, vol. 61, no. 7, pp. 56–66, 2018.
11. A. Fawzi, O. Fawzi, and P. Frossard, "Analysis of classifiers' robustness to adversarial perturbations," *Machine Learning*, vol. 107, no. 3, pp. 481–508, 2018.
12. D. Zügner, A. Akbarnejad, and S. Günnemann, "Adversarial attacks on neural networks for graph data," in *Proceedings of the 24th ACM SIGKDD International Conference on Knowledge Discovery & Data Mining*, 2018, pp. 2847–2856.
13. K. Xu, H. Chen, S. Liu, P.-Y. Chen, T.-W. Weng, M. Hong, and X. Lin, "Topology attack and defense for graph neural networks: An optimization perspective," *arXiv preprint arXiv:1906.04214*, 2019.
14. R. Feinman, R. R. Curtin, S. Shintre, and A. B. Gardner, "Detecting adversarial samples from artifacts," *arXiv preprint arXiv:1703.00410*, 2017.
15. J. H. Metzen, T. Genewein, V. Fischer, and B. Bischoff, "On detecting adversarial perturbations," *arXiv preprint arXiv:1702.04267*, 2017.
16. P. Yang, J. Chen, C.-J. Hsieh, J.-L. Wang, and M. Jordan, "ML-LOO: Detecting adversarial examples with feature attribution," in *Proceedings of the AAAI Conference on Artificial Intelligence*, vol. 34, no. 4, 2020, pp. 6639–6647.
17. C. Agarwal, A. Nguyen, and D. Schonfeld, "Improving robustness to adversarial examples by encouraging discriminative features," in *2019 IEEE International Conference on Image Processing (ICIP)*, IEEE, 2019, pp. 3801–3505.
18. X. Liu, Y. Li, C. Wu, and C.-J. Hsieh, "Adv-BNN: Improved adversarial defense through robust Bayesian neural network," *arXiv preprint arXiv:1810.01279*, 2018.
19. K. Sharma, S. Verma, S. Medya, A. Bhattacharya, and S. Ranu, "Task and model agnostic adversarial attack on graph neural networks," in *Proceedings of the AAAI Conference on Artificial Intelligence*, vol. 37, no. 12, 2023, pp. 15091–15109.
20. F. R. Chung, *Spectral Graph Theory*. American Mathematical Society, 1997, vol. 92.
21. U. von Luxburg, "A tutorial on spectral clustering," *Statistics and Computing*, vol. 17, no. 4, pp. 395–416, 2007.
22. G. H. Golub and C. F. Van Loan, *Matrix Computations*. JHU Press, 2013.
23. W. Cheng, C. Deng, Z. Zhao, Y. Cai, Z. Zhang, and Z. Feng, "Spade: A spectral method for black-box adversarial robustness evaluation," in *International Conference on Machine Learning*, PMLR, 2021, pp. 1814–1824.
24. Y. A. Malkov and D. A. Yashunin, "Efficient and robust approximate nearest neighbor search using hierarchical navigable small world graphs," *IEEE Transactions on Pattern Analysis and Machine Intelligence*, vol. 42, no. 4, pp. 824–836, 2020.

25. A. Ben-Hur, D. Horn, H. T. Siegelmann, and V. Vapnik, "Support vector clustering," *Journal of Machine Learning Research*, vol. 2, pp. 125–137, 2001.
26. W. Jin, Y. Ma, X. Liu, X. Tang, S. Wang, and J. Tang, "Graph structure learning for robust graph neural networks," in *Proceedings of the 26th ACM SIGKDD International Conference on Knowledge Discovery & Data Mining*, 2020, pp. 66–74.
27. Y. Li, W. Jin, H. Xu, and J. Tang, "Deeprobust: A PyTorch library for adversarial attacks and defenses," *arXiv preprint arXiv:2005.06149*, 2020.
28. E. Chien, J. Peng, P. Li, and O. Milenkovic, "Adaptive universal generalized PageRank graph neural network," in *International Conference on Learning Representations*, 2021. Available at <https://openreview.net/forum?id=n6jl7fLxrP>.